IEEE Access
Multidisciplinary | Rapid Review | Open Access Journal

Received April 2, 2020, accepted April 23, 2020, date of publication April 28, 2020, date of current version May 15, 2020.

Digital Object Identifier 10.1109/ACCESS.2020.2990964

Numerical and Experimental Study on Design Optimization of Hybrid Metamaterial Slab for Wireless Power Transmission

WENJIA YANG, SIU-LAU HO, AND WEINONG FU
Department of Electrical Engineering, The Hong Kong Polytechnic University, Hong Kong
Corresponding author: Weinong Fu (eewnfu@polyu.edu.hk)

This work was supported by the Research Grant Council of the Hong Kong SAR Government under Project PolyU 152254/16E, Project G-YBPM, and Project G-YBY7.

ABSTRACT Wireless power transmission (WPT) technique has advanced rapidly in the past two decades. For wireless power transmission distances from 40 to 200 mm, the resonance coupling WPT (R-WPT) technique has surpassed its original inductive coupling counterpart in terms of transmission efficiency. Nevertheless, the power transfer efficiency of a R-WPT system is still lower than that of a wired power transfer system. To increase the power transfer efficiency of a R-WPT system, metamaterial (MM) slabs are inserted between the transmitter and receiver. Moreover, it has recently been validated that a hybrid MM (HMM) slab with different resonance frequency unit cells behaves better than a homogeneous MM slab with identical resonance frequency unit cells in a R-WPT application. However, in the existing HMM slab designs for WPT applications, a trial and error approach, is commonly used to decide the physical and circuit parameters of the HMM slab due to the overwhelmingly high computational cost of numerical simulations using three-dimensional (3-D) finite element method. To overcome the deficiencies of the existing designing methodology and to fully automate the design process, a design-of-experiment (DOE) assisted sequential refinement methodology is proposed by introducing an adaptive surrogate model with tabu search method, for design optimizations of HMM slabs in R-WPT applications. Compared with the existing refinement searching procedures, the salient feature of the proposed one is its bi-directional characteristics, which can refine the searches in the promising sub spaces by intensifying sampling points; and use coarse searches or even discarding the exploitations in the worst sub spaces using some adaptive upper and lower limits of the decision parameters. To validate the feasibility and show the advantages of the proposed methodology, detailed numerical and experimental studies on a case study of a four-coil WPT system working at 13.88 MHz are conducted, and the results have shown that the HMM slab optimized by using the proposed methodology does have better performance in WPT applications when compared to its homogenous counterparts.

INDEX TERMS Adaptive Kriging model, metamaterial, surrogate based optimization, wireless power transmission.

I. INTRODUCTION

Wireless power transmission (WPT) has experienced tremendous progress in the past two decades. Generally, for the applications with wireless transmission distances up to 40-200 mm [1], the resonance coupling technique has surpassed the original inductive coupling one due to a relatively high transmission efficiency in the former. The resonance WPT (R-WPT) technique is developed based on the resonant coupling between two coils, the transmitter and the receiver, that have an identical resonance frequency in the system [2]. Nevertheless, the power transfer efficiency (PTE) of a R-WPT system is still lower than that of a wired power transfer system. To increase both the power transfer efficiency and the transmission distance of a R-WPT system, metamaterial (MM) slabs are inserted between the transmitter and receiver, something like relay coils serving as an intermediate station for power transmission [3], [4]. However, the proposed

The associate editor coordinating the review of this manuscript and approving it for publication was Ruofei Ma.

metamaterial slab, when compared to a relay coil, is much smaller in the device footprint, and hence is more appropriate in applications that have space constraints [5]. Moreover, the performance enhancement by using an optimized metamaterial slab is generally stronger than that by using a relay coil. MM is an artificial material that exhibits extraordinary physical properties that do not exist in nature, and is often fabricated by depositing some metal patterns on dielectric materials using the PCB printing technology [4]. In a R-WPT application, a left-handed MM with both negative permeability and negative permittivity is often used to manipulate the propagating electromagnetic waves and fields to increase the PTE of the system [6]. However, in the frequency band of a R-WPT system, the dimension of the system or device is extremely small compared to the wavelength of the dominating working frequency. The corresponding electromagnetic field can thus be viewed as a quasi-static one [4], and the electric and magnetic fields are virtually decoupled. One can thus manipulate this near-magnetic field using a single negative permeability metamaterial [2]. A metamaterial usually consists of a large number of microscale units or unit cells. Originally, all unit cells of a MM slab in WPT applications are set to be identical to form a periodic structure and a resultant uniform physical property, and hence the MM structure is often regarded as a homogeneous material in macroscale. However, it is proved that a small distortion will not affect the overall property of a periodic structure material, such as an MM structure [7], and moreover a cavity can be created at the centre of the MM slabs to confine the transmitting electromagnetic wave and field; and the PTE of the WPT system can be further enhanced [8]. This type of MM slabs is termed as a hybrid MM (HMM) and the effectiveness of HMM slabs in WPT applications has recently been validated [9]–[12].

However, the analysis and computation of the performance of a metamaterial, including the hybrid metamaterial-based R-WPT system, will face some challenges and bottleneck problems. First, a metamaterial usually consists of a large number of microscale units. To evaluate the performance of a metamaterial-based system or device, one often has to model the entire system instead of modelling only the metamaterial units. However, the node number of the mesh for numerical approach and the degrees of freedoms of a full-wave EM simulation will be too large if one discretizes the entire system or device in the scale of the unit cells. For example, the widely used spiral (Swiss-roll) unit metamaterials for low-frequency near-magnetic field applications usually require an extremely fine mesh. The degrees of freedom will be unacceptable if too many such metamaterial units are included in the computation domain. Secondly, although a metamaterial could be homogenized and can properly be modelled as a bulk or a surface using an equivalent complex permeability and/or permittivity in the near field system, rather than be modelled as an assembly of unit cells, the universal methodology and method to extract the negative equivalent complex permeability and/or permittivity are still developing and unavailable in the current stage for the near field computation of MMs, not to mention the corresponding numerical method. Consequently, an extremely heavy computational cost of a full-wave EM simulations is generally involved in the precise performance evaluations of an HMM slab based WPT system. As a result, in the existing HMM slab designs for WPT applications, a trial and error approach, rather than a full wave EM simulation, is commonly used to decide the physical and circuit parameters of the HMM slab [7], [9]–[12]. Obviously, only very limited portion of the entire design space in the problem can be explored in the optimization process using such an existing approach, and the final design relies heavily on the experience of the designer. To overcome these deficiencies of the existing designing methodology and to fully automate the design process, a DOE assisted sequential refinement method for design optimizations of HMM slabs in R-WPT applications is proposed, examined and validated via both numerical simulations and experimental studies. The proposed search methodology can refine the searches in the promising subspaces; and have a coarse search, or even discard the exploitations in the worst subspaces. Hence, the proposed optimization methodology requires a smaller number of samples to effectively predict a full EM simulation results when compared to a conventional surrogate model, reducing significantly the computational cost of the design optimization process. As a result, a more detailed exploration of the effects of different possible HMM designs in the WPT energy transfer efficiency can be conducted. To validate the proposed optimization methodology, it is applied to optimize the HMM slabs in a conventional four-coil R-WPT system, and the numerical comparisons between the proposed methodology, other types of surrogate models and full EM simulations have revealed that the proposed methodology is able to accelerate the solution speed without any compromise on the solution quality. Both the numerical and the experimental results of an HMM based WPT systems show that the HMM slabs designed by using the proposed methodology outperforms its homogenous counterpart with a PTE enhancement up to 12 %.

II. HYBRID METAMATERIAL FOR NEAR-FIELD ENHANCEMENT

Consider the case when a magnetic field passes through the boundary of two materials with different relative permeability, the normal component of the magnetic flux density B will be continuous

$$B_1^{\perp} = B_2^{\perp} \tag{1}$$

where subscript 1 and 2 stand for two types of materials. On the other hand, consider a small Gaussian loop at the boundary of the two materials, by applying Ampere's Circuital Law, the tangential component of the magnetic field H follows

$$H_1^{\mathrm{P}} - H_2^{\mathrm{P}} = \sum I_{\mathrm{surface}} \tag{2}$$

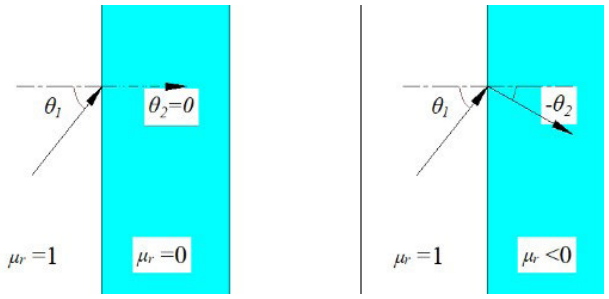

FIGURE 1. Refractive principle of MM with zero and MM with negative μ_r.

If there is no surface current at the boundary (2) becomes

$$\frac{B_1^{\mathrm{P}}}{\mu_1} - \frac{B_2^{\mathrm{P}}}{\mu_2} = 0 \tag{3}$$

In these equations, μ_1 and μ_2 are the relative permeability of the two materials. Combined (1) and (3), the magnetic boundary condition at the interface of the two materials with different permeability can be described as

$$\tan\theta_1 / \tan\theta_2 = \mu_1 / \mu_2 \tag{4}$$

where, θ_1 and θ_2 are the refractive angles at the two sides of refraction, respectively.

As depicted in Fig. 1, negative permeability materials can be used to guide the propagation of waves and fields, and focus the near field of a R-WPT system to increase the system PTE. Consequently, the design of MM has been merged with other types of periodic structures, such as photonic crystals, to form an HMM structure, in order to investigate the possibility for further electromagnetic performance enhancement [9]–[12]. The working principle of the cavity based HMM is an analogy to the bandgap structure in the photonic crystal [13]. Due to the periodic nature in metamaterials, small defects will not affect the overall property of the structure [7]. Thus, the cavity mode is created by inserting abnormal unit cells into the periodic structure, thereby creating a tunnel for a specific frequency of near field to travel through. Due to the fact that unit cells near the cavity all work in the hybridization bandgap, the cavity can confine the near-field and hence enhance the PTE [9]. A typical study has revealed that a more 5% increment of PTE at a transmission distance of over 150 mm using a 6.8 MHz resonance frequency HMM slab [10]. However, in the design of the HMM slabs for WPT applications, to evaluate the PTE of the system and investigate the spatial field distribution, a full time-domain 3-D finite-element method (FEM) simulation procedure is necessary. As explained previously, this is a typical large-scale problem with very fine mesh resolution, and consequently, the FEM simulations of the whole system often involve millions of mesh elements, and the computational cost for one simulation may take several hours. The ensuing high computational cost, which renders the design methodology to inappropriate for optimizing HMM slabs in R-WPT system, is the main shortcoming of the existing field analysis approaches and stochastic population-based optimal algorithms. In most of the existing studies, the trial and error approach or a tuneable device such as a capacitor is commonly used to find the potential HMM designs [9]–[12]. Obviously, a major problem of such design methodology is that only a very limited portion of the design space can be explored, and hence there is no guarantee that the methodology can converge to the global optimal solution, and the design of the HMM slabs is heavily dependent on the experience of the designer.

III. A DOE ASSISTED SURROGATE MODEL AND IMPROVED TABU SEARCH BASED REFINEMENT OPTIMAL METHODOLOGY

In the HMM designs, the unit cells for cavity on the slabs and their surrounding unit cells are set to have different resonance frequencies [11]. Once all the physical parameters for the WPT system are determined, the optimization goal thus becomes finding the best combinations of resonance frequencies of all unit cells in the HMM slabs, in order to obtain the highest PTE of the WPT system. This can be achieved by changing the physical designs of each unit cell, such as the sizes and dimensions, its metallic pattern, and the capacitances of the on-chip capacitors. In the optimization process, the inductances of every unit cell are fixed, so that the mutual inductances between the HMM slabs and the transmitting (Tx) or receiving (Rx) coils are fixed, and hence the resonance frequency of the WPT system will not be distorted when the HMM design changes as the optimization process progresses, and the performance of the WPT system itself maintains at its best at its working frequency. To tune the resonance frequency and hence the permeability of all the unit cells in HMM slabs, the capacitances of the on-chip capacitors are selected as the main control parameters, and the distances between different unit cells are chosen as the secondary decision variables to adapt different geometry scale of the WPT system. Since the microscopic scale resolution of the MM unit cell is extremely high as compared to the physical dimensions of the R-WPT system, a full FEM simulation of the whole system involves millions of mesh elements. For instance, for an MM slab with 0.0035 mm thickness metal structure, the total mesh for the WPT system is more than one million elements using a relatively fine mesh, and more than 30 minutes are needed for the meshing using a 32GB memory computer. Hence, the optimization of the HMM slab is extremely time consuming. In this regard, a DOE assisted surrogate model based on Kriging method with an adaptive searching refinement methodology is proposed to deal with this specific type of problems.

Kriging method is one of the most commonly practiced surrogate models developed as a category in the response surface method and enjoys the merit of more accurate [15]. It can be formulated as [16]:

$$\hat{f}(x) = w_0 + \sum_{i=1}^{N} w_i \exp\left[-c^2 \|x - x_i\|^2\right] \tag{5}$$

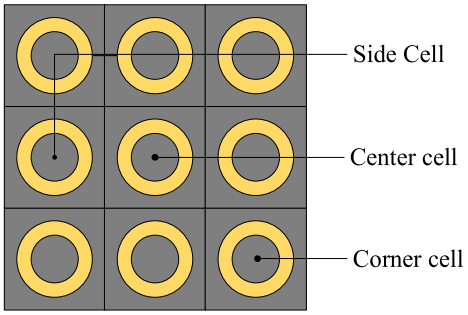

FIGURE 2. Classification of different types of unit cells.

where, $\hat{f}(x)$ is the predicted value of $f(x)$ at observing or sampling point x, w_i $(i = 1, 2, \ldots, N)$ is a weighting factor, c is a correlation parameter, N is the number of sampling points. The accuracy of the reconstructed function $\hat{f}(x)$ depends highly on the values of the weighting factors and the correlation, as well as the way that the observing points to be sampled. To ensure a relatively full exploration of the entire design space with relatively small sampling points, a Latin-Hypercube sampling-based design-of-experiment (DOE) method is employed to determine the positions of the observing points. In the DOE method, the number of samples required to reconstruct the response is related to the number of design parameters [18]:

$$N = cp^s \tag{6}$$

where p is the number of the portions that each design parameter is divided into; c is an adjusting coefficient in the iteration process; and s is the number of the design parameters.

In this paper, a 3 × 3 unit cell HMM slabs are used as just a prototype of the optimization study, and the proposed methodology, just as other optimal algorithms, can be extended to HMM slabs with arbitrary numbers of the unit cells without any limitation on the number of decision parameters. To maintain the symmetrical geometry of the HMM slabs, the unit cells are classified into three different groups, namely the centre cell, the corner cells, and the side cells (Fig. 2). The centre cell has a fixed on-chip capacitance and a fixed resonance frequency which is equal to the working frequency to ensure a maximum near-field transmission at the middle of the HMM slabs. The two main control parameters, the capacitances of four side cells and four corner cells, together with the secondary variables, the distance between different cells, will be optimized to form a cavity at the centre of the slab.

The DOE assisted surrogate models have been widely applied to solve complex 3-D EM problems [17]–[21]. To reduce the number of sampling points required in a DOE, the proposed methodology introduces a multi-start refinement strategy. For example, for the convenience of intuitive explanations, one takes the two capacitors as an example, and the initial design space in this case study for the two capacitors is a two-dimensional (2-D) space formed by the two

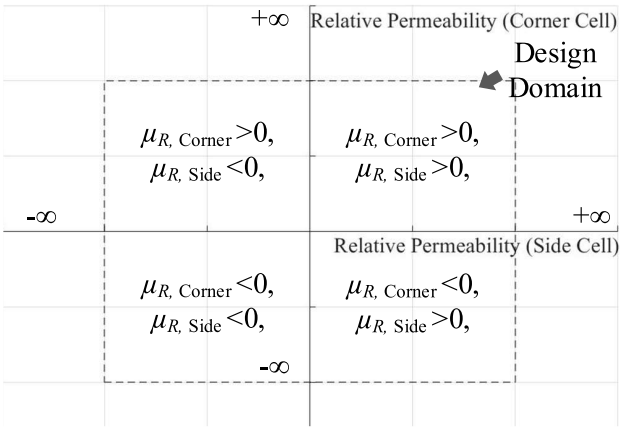

FIGURE 3. Design domain and four subdomains of the two capacitors.

control parameters, the capacitances of the on-chip capacitors of the side cell and the corner cell and the associated resonance frequencies, are depicted in Fig. 3. The proposed multi-start strategy divides this design space into four subspaces based on the values of the relative permeability of the corner cells and the side cells at the working frequency. The design domain is hence divided into four quadrants, which are the positive-positive, positive-negative, negative-positive, and lastly negative-negative quadrants, as illustrated in Fig. 3. For each possible design in the design domain, the capacitance values of its corner cells and side cells will determine the resonance frequencies of these two types of cells, and hence the subdomain the design will fall into.

In each sub space at the k^{th} iteration, the Latin-Hypercube Sampling (LHS) method is used to generate N_i^k sampling points for the Kriging method to construct the local surrogate model of the R-WPT system based on the 3-D FEM evaluations. The initially starting point in each subspace for the first iterative cycle is selected randomly. In the k^{th} iteration, the starting points of the decision parameters in each subspace are selected to be exactly the optimal solutions of the last iteration in that subspace, and the neighbourhood of the starting points is sampled using the LHS method to generate certain number of sampling points, and the objective values of these sampling points will be evaluated using three-dimensional (3-D) FEM. Lastly, the Kriging surrogate model is constructed using all available sampling points from the 1st iteration cycle to the k^{th} iteration cycle, and an improved tabu search method is implemented in each subspace to find the global optimum of the k^{th} iteration and will be iteratively used as the starting point of the next iteration. Compared with the existing refinement searching procedures, the salient feature of the proposed one is its bi-directional characteristics. More specially, the proposed refinement searching methodology refines the searches in the promising sub spaces by intensifying sampling points and gradually pinpoints the exact global optimal solution by using some adaptive upper and lower limits of the decision parameters; coarse searches are

used or exploitations are even discarded in the worst sub spaces. The upper and lower bounds of the decision parameters, h, of two consecutive iterations, $k+1$ and k, decreases exponentially via the predefined adaptive parameters α_1 as:

$$h_{kriging}^{k+1} = h_{kriging}^{k} \times \alpha_1, \quad 0 < \alpha_1 < 1 \tag{7a}$$

Similarly, the reduction of the number of sample points in the subspace with relatively lower rank, $N_{\text{worst objective}}$, of two consecutive iterations, $k+1$ and k, is updated using a predefined shrinking ratio, α_2, using the following round function:

$$N_{\text{worst objective}}^{k+1} = round(N_{\text{worst objective}}^{k} \times \alpha_2) \tag{7b}$$

Once the local surrogate model for each sub space is constructed, any optimal algorithm can be used readily to solve the corresponding optimization problem. However, an improved tabu search method is introduced and used due to its simplicity and fast convergence speed. The major improvement in the proposed tabu search algorithm when compared to the existing one in [14] is the generating mechanism for the neighbourhood solutions. The search space for the improved tabu search method in each iteration cycle is the same as the sampling space for the surrogate model, rather than the whole one; and the step size for each parameter in the tabu search is 1/100 of the search space, so that the entire space will be extensively explored. The reason that one selects the step seize of 1/100 of the search space is that the change in the capacitance values will not significantly affect the objective value if the step size is smaller than this limit, other thing being equal. Because the computation of the objective function values using a Kriging model is much faster than that using an FEM simulation, the tabu search process for each iteration cycle can be completed within a very short time. Moreover, in the proposed improved tabu search method, the so far searched best solution in each sub region of the feasible space is recorded and used to guide the generation of new neighbourhood solutions. A weighted aggregation of the best objective functions from all subspaces is used to guide the search of the tabu method, and the updating of both step size and the searching position are given by:

$$\begin{aligned} h_{tabu}^{k+1} &= h_{kriging}^{k+1} \times 0.01 \\ x_i^{n+1} &= x_i^n + r\Delta x_i^{n+1} + (1-r)\sum_{j=1}^{M} w_j x_j^{best} \end{aligned} \tag{8}$$

where n is the number of iterations in the tabu process, j is the j^{th} subspace, r is a random parameter which is uniformly distributed in [0 1]. To consider the closeness of an optimal point, for example x_j^{best}, in different subspaces, the weighed parameter w_j is inversely proportional to the distance of the point, x_i^n, in relation to x_j^{best}.

After the optimization of each subspace in each cycle using the improved tabu search method, the subspaces will then be sorted based on the performance parameter values, and the numbers of sample points of the sub spaces with the best and worst performances will be automatically intensified and reduced, respectively, in the next iteration.

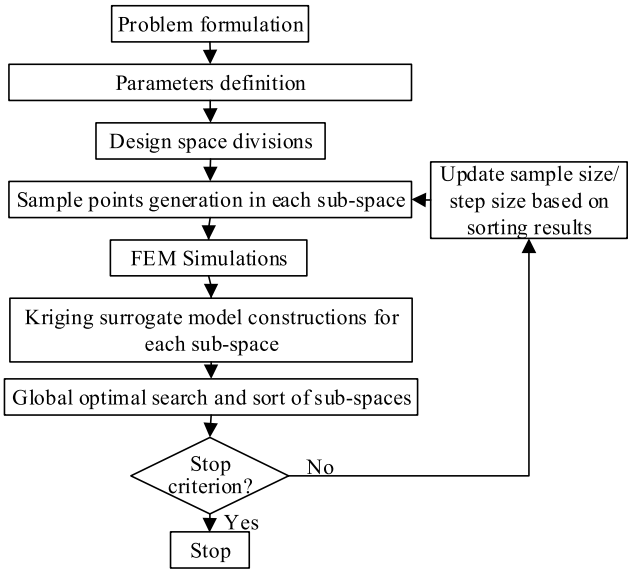

FIGURE 4. Flow chart of the proposed methodology.

The iterative procedure of the proposed optimization methodology will continue until the differences or errors in the searched best objective function values for each subspace in the two consecutive iterative cycles are smaller than a predefined tolerance. To facilitate the implementation of the proposed optimization methodology, its flow chart is given in Fig. 4.

IV. NUMERICAL STUDY

The proposed methodology is applied to optimize the HMM slabs of a four-coil 13.88 MHz R-WPT system. 13.88 MHz is chosen as the working frequency because in the experimental setup it is found that 13.88 MHz is the frequency that is only obtainable (the closest one to 13.56 MHz, one of the frequency centre in ISM band) by using integer incremental values of capacitances. However, to facilitate a fair comparison between the simulated results and the experimental ones, the working frequency is slightly varied. The arrangement of the prototype is shown in Fig. 5. The distance between Tx and Rx coils is 150 mm, and the two coils are identical copper coils with a 60 mm radius and a 30 mm spiral length. The copper coils are set as 1 mm width square helix for a faster simulation. One 23.2 pF capacitor is connected to the ends of the Tx/Rx coils to tune the resonance frequency of the coils to 13.88 MHz, and an HMM slab is placed right at the centre of the system. In the unit cell of the HMM slab, a 15-turn copper coil with 0.0035 mm thickness (0.0035mm is one of the standard thickness in PCB printing technology), 0.5 mm width and 0.5 mm spacing is deposited on one side of the surface of the 1.6 mm thick, 37.2 mm wide FR-4 substrate, and an on-chip capacitor is connected at the ends of the metallic pattern for resonance frequency calibration.

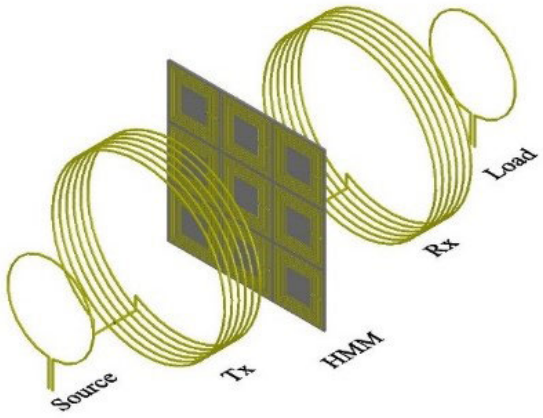

FIGURE 5. The prototype R-WPT system under optimization.

TABLE 1. Circuit parameters of two experiments.

	Numerical	Actual
Inductance (MM)	9.9 μH	NIL
Inductance (Source)	81 nH	160 nH
Inductance (Tx/Rx)	5.9 μH	23.3 μH
Capacitance (Tx/Rx)	23.2 pF	6 pF

Table 1 summarizes all circuit parameters of the numerical experiments and the experimental studies. In the experimental study, it is hard to keep the copper wire loosely as that is done in the simulation cases, and the copper wire is tightly wounded on the plastic tubes. Consequently, the inductances of the coils in the experimental study are much higher than those of the numerical simulation computations. Nevertheless, the resonance frequency, as well as the distance between the source and load coils, are kept as the same for both cases to ensure a fair comparison.

The goal of the design optimization is to maximize the PTE, measured using the transmitting coefficient S_{21} [11] between the two ports defined at the source and the load coils with an impedance of 50 Ω, of the system, from:

$$\begin{aligned} &\max PTE(x_i) = |S_{21}|^2 \\ &\text{s.t. } x_i \subseteq [x_i^{\min}, x_i^{\max}] \quad (i = 1 \text{ or} 2) \end{aligned} \tag{9}$$

The 3-D FEM simulation is used to compute the system performance at the sampling points and one simulation costs about one hour for more than 1 million mesh elements on a desktop with Intel® i5-6600 3.30GHz CPU and 32GB DDR4 RAM, and the mesh size is 0.0035 mm at the surface of the HMM slab, and gradually increase to 1 mm for the rest of the 3D model. To determine the range of the on-chip capacitance, unit cell FEM simulations are conducted to examine its permeability in different capacitance values at the working frequency using an effective homogeneous medium method [5]. It is observed that when the capacitance value is not within the range of 12 pF to 16 pF, the permeability of the unit cell remains constant, and variations will no longer influence the system PTE. Hence, the two main or primary design parameters, the on-chip capacitances of the corner and side unit cells, are set in the range of 12 pF to 16 pF for sampling, in order to reduce the design space. The starting points of four sub spaces of the capacitances are hence located at: 13 pF-13 pF, 13 pF-15 pF, 15 pF-13 pF and 15 pF-15 pF, and the initial number of samples of LHS is 16, with an initial step size of 1 pF and adaptive parameters, α_1 and α_2, in (7), of 0.5 and 0.6, respectively, selected by using a trial and error approach. In the iterative process of the proposed methodology, from the second iterations onward, only three sub-spaces for the capacitors are active, and one subspace (the 15 pF-15 pF subspace) is discarded due to its extremely poor performances of all candidates in that specific subspace. Moreover, the additional sampling points for the worst subspace eventually become only 12% of all additional sampling points of all subspace when the optimization procedure terminates at the fifth iteration.

TABLE 2. Comparisons of different surrogate models.

	Optimal solution (Capacitances)	PTE (and relative error)	No. of FEM runs
Proposed	(11.1pF,14.9pF)	15.4% (4%)	188
SKE	(14.3pF,9.9pF)	3.2% (80%)	188
LI	(11.0pF,11.0pF)	5.6% (65%)	220
Full FEM	(11.1pF,14.9pF)	16% (0%)	400

To showcase the accuracy of the proposed refinement methodology, a comparative study, using the proposed method; a sequential Kriging based method excluding the proposed refinement procedure (SKE), other things being equal; and a linear interpolation (LI) is conducted. The numerical results have shown that both the SEK and the LI methods have faced premature convergence to non-optima due to the significantly large errors of the models, while the proposed method is able to gradually pinpoint the exact optimum. The detailed results are compared in Table 2. Since it is infeasible to optimize this case study by using a full EM simulation directly, a roughly accurate surrogate model is reconstructed to represent the entire design space by using a more sampling points model, that is a 400-sample points DOE model. Using this computational heavy DOE model, the final optimized PTE is 15.97%, very close to the optimal solution of the proposed methodology; and however, the time taken for the optimization using this heavy DOE model is more than two times of the proposed methodology, not to mention the time for a full EM simulation without any help from a surrogate model. Moreover, due to the independence of each subspace, in the proposed method, a parallel computing technique can be employed to further increase the solution speed. Fig. 6 compares the objective function values of the best candidates in the five iterative cycles using a full FEM

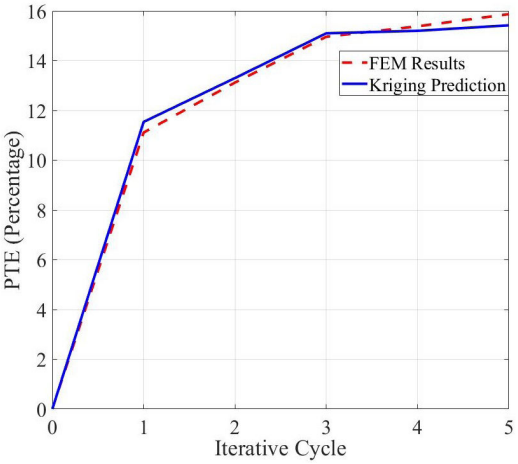

FIGURE 6. Comparison of a full FEM simulation and the proposed Kriging model on the calculated objective function values of the best candidates in the five iterative cycles.

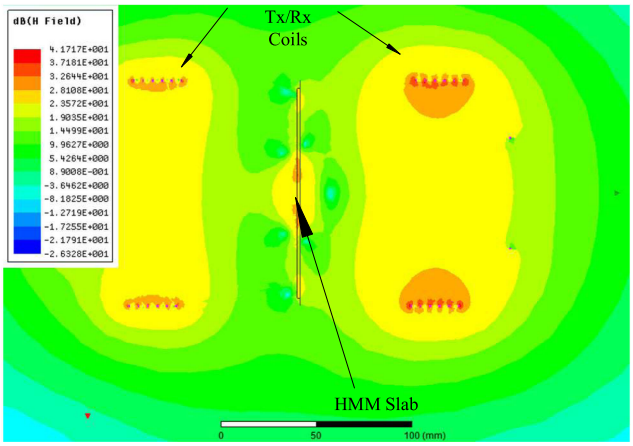

FIGURE 7. Propagation of *B* field in HMM assisted WPT system.

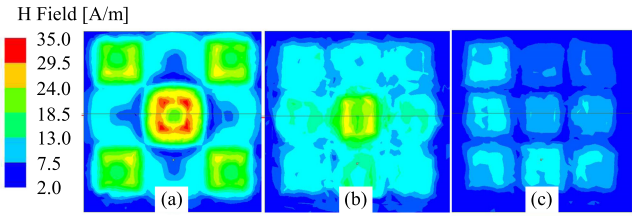

FIGURE 8. *B*-field distributions for (a) proposed HMM slab, (b) HMM slab with only one defect at centre, and (c) Homogenous slab.

simulation and the corresponding kriging models. The two results agree very well, and the error is within 5%, indicating the proposed method can accurately reconstruct the design space, especially at the function optima.

To show the magnetic field enhancement effects of different HMM structures, Fig. 7 gives the log scale plot of the magnetic field distribution of the HMM assisted WPT system. From this colour map plot, it can be clearly seen that there is a very narrow tunnel created at the centre of the HMM slab, which in turn manipulates the propagation of the magnetic field as well as the transmission of the electric energy. Moreover, the field at the receiving coil Rx is comparable in magnitude to the field at the transmitting coil Tx, indicating a high PTE due to the application of the HMM slab.

To further investigate the performance as well as the advantage of the proposed HMM slab as compared to other geometrical MM slabs in existing WPT applications, Fig. 8 (a)∼(c) give intuitively the magnetic field distributions on one side of a HMM slab at the *xoy* plane perpendicular to the transmission direction for the proposed HMM slab, the HMM slab with only one defect unit cell at the centre, and the homogeneous MM slab with all identical unit cells, respectively. The excitation sources for all three cases are the same. From these numerical results, it can be obviously concluded that:

(1) The magnetic near field is confined in the cavity created by the HMM slab in both case 1 and case 2;

(2) However, a stronger B-field is observed in the optimized HMM slab as compared to the HMM slab of case 2, and hence a higher PTE is expected;

(3) The PTEs for the three cases are sequentially 15.38%, 11.5% and 3.8%, which are also in good agreements with the *B*-field distributions.

V. EXPERIMENTAL VERIFICATION

To experimentally validate the feasibility and the performance of the proposed optimized HMM slab, a series of R-WPT experimental studies are conducted. The experimental setup follows the FEM simulation exactly, and the prototype is given in Fig. 9. As explained in the previous session of the paper, in the system both Tx and Rx coils have an inductance of 23.3 μH, measured using a high-frequency LCR meter, and are connected to a 6 pF capacitor to fine tune the resonance frequencies. Moreover, it is found that the currents in the coils have no phase difference to the applied voltages at 13.88 MHz when measured using a current probe connected with a high-performance oscilloscope, and hence 13.88 MHz is the resonance frequency. A 1V peak-to-peak AC voltage and a 5V peak-to-peak AC voltage are, respectively, applied to the source coil and the induced voltage (*IV*) at the load coil is measured in three cases:

1) Without any MM slab;

2) With a homogeneous slab that has all unit cells working in resonance at 13.9 MHz at the middle of the Tx and Rx coils;

3) The proposed HMM slab with three different types of unit cells at the middle of the Tx and Rx coils.

Because the load condition does not change for all three cases, the enhancement in PTE due to the addition of the MM slab is determined using the ratio between the measured voltages at the Rx end when there is MM slab, $V_{\text{with MM}}$, to that of where these is no MM slab, $V_{\text{w/oMM}}$:

$$\Delta PTE = (V_{\text{with MM}}/V_{\text{w/oMM}})^2 \tag{10}$$

The experimental results are given in Table 3. It can be seen that there is an increment of 120% PTE enhancement when

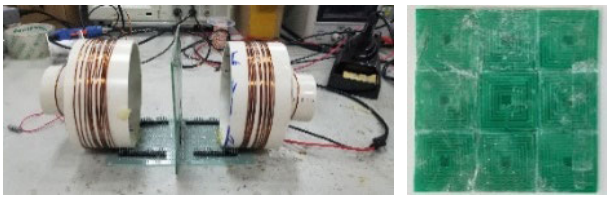

(a) (b)

FIGURE 9. (a) Experimental setup (side view). (b) Actual HMM slab.

TABLE 3. Experimental results.

	Source P-to-P 1V			Source P-to-P 5V		
	Case 1	Case 2	Case 3	Case 1	Case 2	Case 3
IV	68.4mV	85.6mV	103mV	0.82V	1.07V	1.25V
ΔPTE	/	56.6%	126.8%	/	70.3%	132.4%

the proposed HMM slab is used, which is about twice larger than that when a uniform MM slab is used; and in both the high and low voltage excitations cases, the results are almost consistent. These results quantitatively illustrate the success of the proposed method in the optimization of an HMM slab.

VI. CONCLUSION

In this paper, a DOE assisted surrogate and improved tabu search based sequential refinement method for design optimization of MM structures in R-WPT systems is proposed. By utilizing the surrogate method to replace the time-consuming 3-D FEM simulations, the solution time required to find the best objective values is significantly reduced, and hence an automated optimization can be performed. The numerical results indicate that, compared to the conventional surrogate method, the proposed one is able to reconstruct a sufficiently accurate surrogate model; and compared to a full DOE approach, the computational burden of the proposed methodology is very low. Moreover, the experimental verification results indicate the HMM slab obtained by using the proposed method is indeed better than an HMM slab without any optimization.

REFERENCES

[1] T. S. Pham, A. K. Ranaweera, V. D. Lam, and J.-W. Lee, "Experiments on localized wireless power transmission using a magneto-inductive wave two-dimensional metamaterial cavity," *Appl. Phys. Express*, vol. 9, no. 4, Apr. 2016, Art. no. 044101.

[2] Z. Zhen and P. Hongliang, "Wireless power transfer—An overview," *IEEE Trans. Ind. Electron.*, vol. 66, no. 2, pp. 1044–1058, May 2019.

[3] F. Lu, H. Zhang, and C. Mi, "A review on the recent development of capacitive wireless power transfer technology," *Energies*, vol. 10, no. 11, pp. 1752–1781, 2017.

[4] H. Guan, L. Liu, S. Yang, and X. Chen, "Efficiency enhancement of wireless power transfer system by using resonant coil and negative permeability metamaterial," *Int. J. Appl. Electromagn. Mech.*, vol. 59, no. 2, pp. 647–655, Mar. 2019.

[5] H. Guo, Z. Sun, and C. Zhou, "Practical design and implementation of metamaterial-enhanced magnetic induction communication," *IEEE Access*, vol. 5, pp. 17213–17229, 2017.

[6] K. Sun, R. Fan, X. Zhang, Z. Zhang, Z. Shi, N. Wang, P. Xie, Z. Wang, G. Fan, H. Liu, C. Liu, T. Li, C. Yan, and Z. Guo, "An overview of metamaterials and their achievements in wireless power transfer," *J. Mater. Chem. C*, vol. 6, no. 12, pp. 2925–2943, 2018.

[7] H. Nguyen Bui, T. Son Pham, J.-S. Kim, and J.-W. Lee, "Field-focused reconfigurable magnetic metamaterial for wireless power transfer and propulsion of an untethered microrobot," *J. Magn. Magn. Mater.*, vol. 494, Jan. 2020, Art. no. 165778.

[8] N. Kaina, F. Lemoult, M. Fink, and G. Lerosey, "Ultra small mode volume defect cavities in spatially ordered and disordered metamaterials," *Appl. Phys. Lett.*, vol. 102, no. 14, Apr. 2013, Art. no. 144104.

[9] A. L. A. K. Ranaweera, C. A. Moscoso, and J.-W. Lee, "Anisotropic metamaterial for efficiency enhancement of mid-range wireless power transfer under coil misalignment," *J. Phys. D, Appl. Phys.*, vol. 48, no. 45, Nov. 2015, Art. no. 455104.

[10] Y. Cho, S. Lee, D.-H. Kim, H. Kim, C. Song, S. Kong, J. Park, C. Seo, and J. Kim, "Thin hybrid metamaterial slab with negative and zero permeability for high efficiency and low electromagnetic field in wireless power transfer systems," *IEEE Trans. Electromagn. Compat.*, vol. 60, no. 4, pp. 1001–1009, Aug. 2018.

[11] A. L. A. K. Ranaweera, T. P. Duong, and J.-W. Lee, "Experimental investigation of compact metamaterial for high efficiency mid-range wireless power transfer applications," *J. Appl. Phys.*, vol. 116, no. 4, Jul. 2014, Art. no. 043914.

[12] Y. Zhang, H. Tang, C. Yao, Y. Li, and S. Xiao, "Experiments on adjustable magnetic metamaterials applied in megahertz wireless power transmission," *AIP Adv.*, vol. 5, no. 1, Jan. 2015, Art. no. 017142.

[13] B. H. Wang, W. Yerazunis, and K. H. Teo, "Wireless power transfer based on metamaterials," in *Wireless Power Transfer Algorithms, Technologies and Applications in Ad Hoc Communication Networks*. Springer, 2016, pp. 31–53.

[14] S. L. Ho and S. Yang, "Multiobjective synthesis of antenna arrays using a vector tabu search algorithm," *IEEE Antennas Wireless Propag. Lett.*, vol. 8, pp. 947–950, 2009.

[15] Z. Xiaobo, "Comparison of response surface method and kriging method for approximation modeling," in *Proc. 2nd Int. Conf. Power Renew. Energy (ICPRE)*, Chengdu, China, Sep. 2017, pp. 66–70.

[16] K. Hamza, M. Aly, and H. Hegazi, "A kriging-interpolated level-set approach for structural topology optimization," *J. Mech. Design*, vol. 136, no. 1, Jan. 2014, Art. no. 011008.

[17] T. Long, D. Wu, X. Chen, X. Guo, and L. Liu, "A deterministic sequential maximin latin hypercube design method using successive local enumeration for metamodel-based optimization," *Eng. Optim.*, vol. 48, no. 6, pp. 1019–1036, Jun. 2016.

[18] G. Lei, X. M. Chen, J. G. Zhu, Y. G. Guo, W. Xu, and K. R. Shao, "Multiobjective sequential optimization method for the design of industrial electromagnetic devices," *IEEE Trans. Magn.*, vol. 48, no. 11, pp. 4538–4541, Nov. 2012.

[19] G. Lei, K. R. Shao, Y. Guo, J. Zhu, and J. D. Lavers, "Improved sequential optimization method for high dimensional electromagnetic device optimization," *IEEE Trans. Magn.*, vol. 45, no. 10, pp. 3993–3996, Oct. 2009.

[20] X. Liu and W. N. Fu, "A dynamic Dual-Response-Surface methodology for optimal design of a permanent-magnet motor using finite-element method," *IEEE Trans. Magn.*, vol. 52, no. 3, pp. 1–4, Mar. 2016.

[21] Y. Zhang, S. L. Ho, and W. Fu, "Applying response surface method to oil-immersed transformer cooling system for design optimization," *IEEE Trans. Magn.*, vol. 54, no. 11, Nov. 2018, Art. no. 8401705

WENJIA YANG received the B.Sc. degree in electrical and electronics engineering from Nanyang Polytechnical University, Singapore, in 2014. He is currently pursuing the Ph.D. degree in electrical engineering with The Hong Kong Polytechnic University, Hong Kong.

His research interests include optimization methods for electromagnetic devices, numerical methods for electromagnetic field computation, and simulation methods for electromagnetic field.

SIU-LAU HO received the B.Sc. and Ph.D. degrees in electrical engineering from The University of Warwick, Coventry, U.K., in 1976 and 1979, respectively. He joined The Hong Kong Polytechnic University, Hong Kong, in 1979, where he is currently the Chair Professor and an Associate Vice President. Since joining the university, he has been working actively with local industry, particularly in railway engineering. He is currently the holder of several patents and has authored over 250 conference papers and over 300 articles published in leading journals, mostly in the IEEE TRANSACTIONS and IET proceedings. His research interests include design optimization of electromagnetic devices, the application of finite elements in electrical machines, phantom loading of machines, and railway engineering.

Dr. Ho is also a member of the Hong Kong Institution of Engineers.

WEINONG FU received the B.Eng. degree from the Hefei University of Technology, Hefei, China, in 1982, the M.Eng. degree from the Shanghai University of Technology, Shanghai, China, in 1989, and the Ph.D. degree from The Hong Kong Polytechnic University, Hong Kong, in 1999, all in electrical engineering.

He is currently a Professor with The Hong Kong Polytechnic University. Before joining the University, in 2007, he was one of the key developers with Ansoft Corporation, Pittsburgh, PA, USA. He has about seven years of working experience with Ansoft, focusing on the development of the commercial software Maxwell. He has authored or coauthored more than 200 articles in refereed journals. His current research interests mainly include numerical methods of electromagnetic field computation, optimal design of electric devices based on numerical models, applied electromagnetics, and novel electric machines.